Ribosome display of mammalian receptor domains

Bernhard Schimmele, Nico Gräfe and Andreas Plückthun[1]

Biochemisches Institut der Universität Zürich, Winterthurer Strasse 190, CH-8057 Zürich, Switzerland

[1]To whom correspondence should be addressed.
E-mail: plueckthun@bioc.unizh.ch

Many mammalian receptor domains, among them a large number of potential therapeutic target proteins, are highly aggregation-prone upon heterologous expression in bacteria. This severely limits functional studies of such receptor domains and also their engineering towards improved properties. One of these proteins is the Nogoreceptor, which plays a central role in mediating the inhibition of axon growth and functional recovery after injury of the adult mammalian central nervous system. We show here that the ligand binding domain of the Nogoreceptor folds to an active conformation in ternary ribosomal complexes, as formed in ribosome display. In these complexes the receptor is still connected, via a C-terminal tether, to the peptidyl tRNA in the ribosome and the mRNA also stays connected. The ribosome prevents aggregation of the protein, which aggregates as soon as the release from the ribosome is triggered. In contrast, no active receptor was observed in phage display, where aggregation appears to prevent incorporation of the protein into the phage coat. This strategy sets the stage for rapidly studying defined mutations of such aggregation-prone receptors *in vitro* and to improve their properties by *in vitro* evolution using the ribosome display technology.
Keywords: *in vitro* evolution/nogo receptor/protein aggregation/protein folding/ribosome display

Introduction

Many proteins of mammalian origin are highly aggregation-prone upon heterologous expression, including a large number of potential therapeutic target proteins. These include in particular mammalian receptor domains, which can rely on the complex folding machinery of the eukaryotic cell for secreted proteins (Ellgaard *et al*., 1999) and on glycosylation to improve their solubility (Wyss *et al*., 1995) and stability (Wormald and Dwek, 1999). In contrast, combinatorial selection technologies such as phage display and ribosome display do not provide this environment, as phage display exploits the pathway of bacterial secretion, whereas ribosome display occurs in an *in vitro* translation extract. Both methods are powerful tools for the identification of proteins that bind to a given target molecule and also for the directed evolution of proteins towards improved properties such as binding affinity and stability. Even though these technologies are well established for peptides, antibody fragments and other classes of proteins that are expressed at least to some level in soluble and functional form in

prokaryotic expression systems (Dunn, 1996; Hanes and Plückthun, 1997; Binz *et al*., 2004), other mammalian proteins may not be amenable to these display technologies. Even the investigation of point mutants of such receptors is laborious, as they have to be expressed and tested in eukaryotic systems.

An important class of mammalian receptor domains being involved in a large variety of different interactions is the family of extracellular leucine-rich repeat (LRR) domains (Kobe and Kajava, 2001). Despite their important role and crucial participation in a number of diseases, structural und functional investigations of these domains have proven very difficult, as their heterologous expression in *Escherichia coli* has often only yielded aggregated protein and refolding attempts for members of this class have achieved only very limited success (Hering *et al*., 1996; Lobel *et al*., 2002).

One member of particular interest in this class of proteins is the Nogoreceptor, which interacts with several myelin-associated proteins responsible for inhibiting axonal regeneration after injury in the adult mammalian central nervous system (CNS). Initially, it had been identified as a binding site for the short 66-amino acid extracellular domain of Nogo, termed Nogo-66 (Fournier *et al*., 2001). Nogo is a potent inhibitor of axonal sprouting and functional recovery after spinal chord injury (Chen *et al*., 2000; GrandPre *et al*., 2000). Recent findings suggest the Nogoreceptor to be a point of convergence in signal transduction for several of these inhibitors, indicating that this receptor is indeed a key player in regulating axonal regeneration and plasticity in the adult CNS (McGee and Strittmatter, 2003). The Nogoreceptor is a glycosylphos-phatidylinositol (GPI)-anchored receptor and represents a typical member of the class of extracellular LRR domains. The LRR core region is represented by 8.5 LRR modules, flanked by cysteine-rich N-terminal and C-terminal 'capping' modules, which both contain two disulfide bridges (He *et al*., 2003). The core region is glycosylated with sugar moieties modifying Asn82 and Asn179. A unique C-terminal region of 100 amino acids follows the LRR domain, which is not required for Nogo-66 binding, but plays a role in the interaction with the coreceptor p75 (Wang *et al*., 2002). The LRR domain of the Nogoreceptor has been found to be necessary and sufficient for binding to Nogo-66 (Fournier *et al*., 2002). Importantly, soluble Nogoreceptor–Fc fusion protein has been found to antagonize the growth-inhibiting effects of Nogo in *in vitro* neurite outgrowth assays. Because of the great interest in attempting to stimulate axonal regrowth after spinal chord injuries or stroke, the Nogoreceptor and its ligands represent important drug targets for modulating axonal regeneration. The Nogoreceptor is therefore an especially interesting target for protein engineering and directed protein evolution with the potential of creating variants of higher affinity or stability.

We examined whether ribosome display technology can be applied to such mammalian receptors, even though their heterologous expression in bacteria does not yield natively folded

protein. We were not only able to obtain soluble ternary complexes of RNA, ribosome and receptor domains, but also to reconstitute the interaction between Nogoreceptor and Nogo-66 *in vitro*. In contrast, we did not observe functionally displayed Nogoreceptor protein in a standard phage display system. This finding paves the way for evolving receptor domains with improved properties for developing them into drugs. Moreover, we show that the established assay can be used as a versatile screening tool for studying structure–function relationships *in vitro* on a very rapid time-scale.

Materials and methods

Preparation of plasmids and mRNA

Nogo-66 fusion constructs. A full-length clone of Nogo-A (HUGE database: KIAA0886; GenBank accession No. AB020693) was generously provided by the Kazusa DNA Research Institute. Plasmid pBMS053 encoding a C-terminal fusion of the extracellular domain of Nogo-A (Nogo-66, residues 1055–1120) (GrandPre *et al.*, 2000) to protein D (residues T20–V109 of bacteriophage l gpD) (Yang *et al.*, 2000) with an N-terminal Avi-tag and a C-terminal His-tag is a derivative of pAT221, a version of pAT222 (GenBank accession No. AY327137) with a different reading frame. The Nogo-66 gene fragment was polymerase chain reaction (PCR) amplified and ligated into the *Bam*HI/*Hin*dIII sites of pAT221.

Plasmid pBMS043 encoding a C-terminal fusion of Nogo-66 to *E.coli* thioredoxin (GeneBank accession No. M26133) with an N-terminal His-tag is a derivative of pAT194 (P.Forrer, unpublished work), which is derived from pQE30, but contains a gene fragment coding for protein D after the His-tag followed by unique restriction sites. The thioredoxin gene fragment was amplified and ligated into the *Nco*I/*Bam*HI sites of pAT194 replacing the protein D gene fragment. The PCR-amplified fragment coding for Nogo-66 was inserted between the *Bam*HI/*Hin*dIII sites at the 3′-end of the thioredoxin gene.

Nogoreceptor variants. Macaca fascicularis Nogoreceptor cDNA (GenBank accession No. AB045987) was a kind gift from the National Institute of Infectious Diseases, Japan. For ribosome display, Nogoreceptor variants were cloned into plasmid pRDV2, a derivative of pRD-n1n2_2 (Matsuura and Plückthun, 2003) with a T7 promoter introduced. A gene fragment encoding the ligand binding domain of the macaque Nogoreceptor (residues 24–331) comprising the N-terminal flanking region (LRR-NT), the LRR core region, the C-terminal LRR flanking region (LRR-CT) and an additional short overhang, was inserted in front of the protein D (pD)-linker via *Nco*I and *Bam*HI after PCR amplification. We had previously substituted residues C316 and L329 in the overhang by the respective residues of the human Nogoreceptor. The final PCR amplification resulted in construct NR (Figure 2).

To generate a variant in which the two free cysteines at positions 80 and 140 in the LRR core region are replaced by the respective consensus residues at each position (C80L and C140N), PCR-directed mutagenesis was performed resulting in construct NRC⁻. Deletion mutant NRC⁻ΔLRR-CT lacking the C-terminal LRR-flanking region comprises residues 24–260 and both consensus mutations. Deletion mutant LRR-CT comprises only the C-terminal LRR flanking region (residues 261–314). mRNA of all variants was produced by

in vitro transcription and purified as described previously (Schaffitzel *et al.*, 2001).

For phage display, gene fragments NR and NRC⁻ were PCR amplified with oligonucleotides GGAAAAAGCTCTT-CACCCCTGTTACCAAAGCCGACTACAAAGATGCAGC-CCCGTGCCCAGGCG and GGAAAAGAATTCCCCCAGC-GGCTCCTCGTCGG introducing the restriction sites *Eco*RI at the 3′-end and *Sap*I at the 5′-end, which is located within the *phoA* signal sequence, the remaining portion of the *phoA* signal sequence and the N-terminal FLAG-tag. The fragments were then cloned into the phagemid vector pMorph7 (Morphosys AG), where the construct is placed between a *phoA* signal sequence and the C-terminal domain of the gene 3 protein (g3p). As a control for the binding competency of the NR and NRC⁻ displaying phage, we also prepared phages displaying the single-chain Fv antibody aIFv1, which binds specifically to Nogo-66 and which had previously been obtained by phage panning of the HuCAL library (Morphosys) (Knappik *et al.*, 2000) against different Nogo-66 fusion proteins (B.Schimmele, unpublished results).

Human biglycan cDNA was kindly provided by the Mammalian Gene Collection (clone MGC_19). The gene fragment encoding the core protein (residues 60–368) was PCR amplified as two overlapping fragments, because the gene contains an internal *Nco*I site and the two gene fragments were simultaneously ligated into pRDV2 after restriction with *Nco*I/*Hin*cII and *Hin*cII/*Bam*HI.

Preparation of Nogo-66 fusion proteins

Nogo-66 fusion proteins were expressed as inclusion bodies in *E.coli* C41 (pREP4) (Miroux and Walker, 1996). Expression was continued for 4 h after induction with 1 mM IPTG at 37°C. Cells were collected by centrifugation, resuspended in 50 mM Tris–HCl (pH 8.0), 150 mM NaCl, 4 mM MgCl₂, 20 µg/ml DNase I and lysed with an Emulsiflex-C5 (Avestin). Inclusion bodies were collected by centrifugation and washed three times with 50 mM Tris–HCl (pH 8.0), 150 mM NaCl, 1% Triton. Inclusion bodies were then solubilized with 6 M GdnHCl, 50 mM Tris–HCl, 150 mM NaCl (pH 8.0) and, after centrifugation, proteins were purified on a Ni-NTA column under denaturing conditions according to the manufacturer's instructions (Qiagen, Germany). After purification, DTT was added to a final concentration of 50 mM. Refolding was performed by fast dilution from a 650 µM protein stock solution into 50 mM Tris–HCl, 150 mM NaCl, pH 8.5.

For coating of paramagnetic polystyrene beads (M-270-Epoxy, Dynal Biotech), fusion proteins were extensively dialysed against PBS (pH 8.0). Soluble refolded fusion protein at a final concentration of 14 µM in PBS in 1 M ammonium sulfate was rotated for 60 h at 4°C with 2×10^8 beads/ml. Beads were prepared and blocked according to the manufacturer's instructions. Coated beads were stored at 4°C in PBS (pH 8.0), 0.002% Tween-20 for no longer than 1 week. For inhibition studies protein was rebuffered into WBKT buffer (see below) on a NAP-5 column (Amersham Biosciences) after refolding by fast dilution.

Size-exclusion chromatography

Refolded protein samples at a concentration of 20 µM in 50 mM Tris, 150 mM NaCl, pH 8.5 were applied to a Superdex 200 column (Amersham Biosciences) and the elution profiles were monitored by measuring the absorbance at 280 and 230 nm.
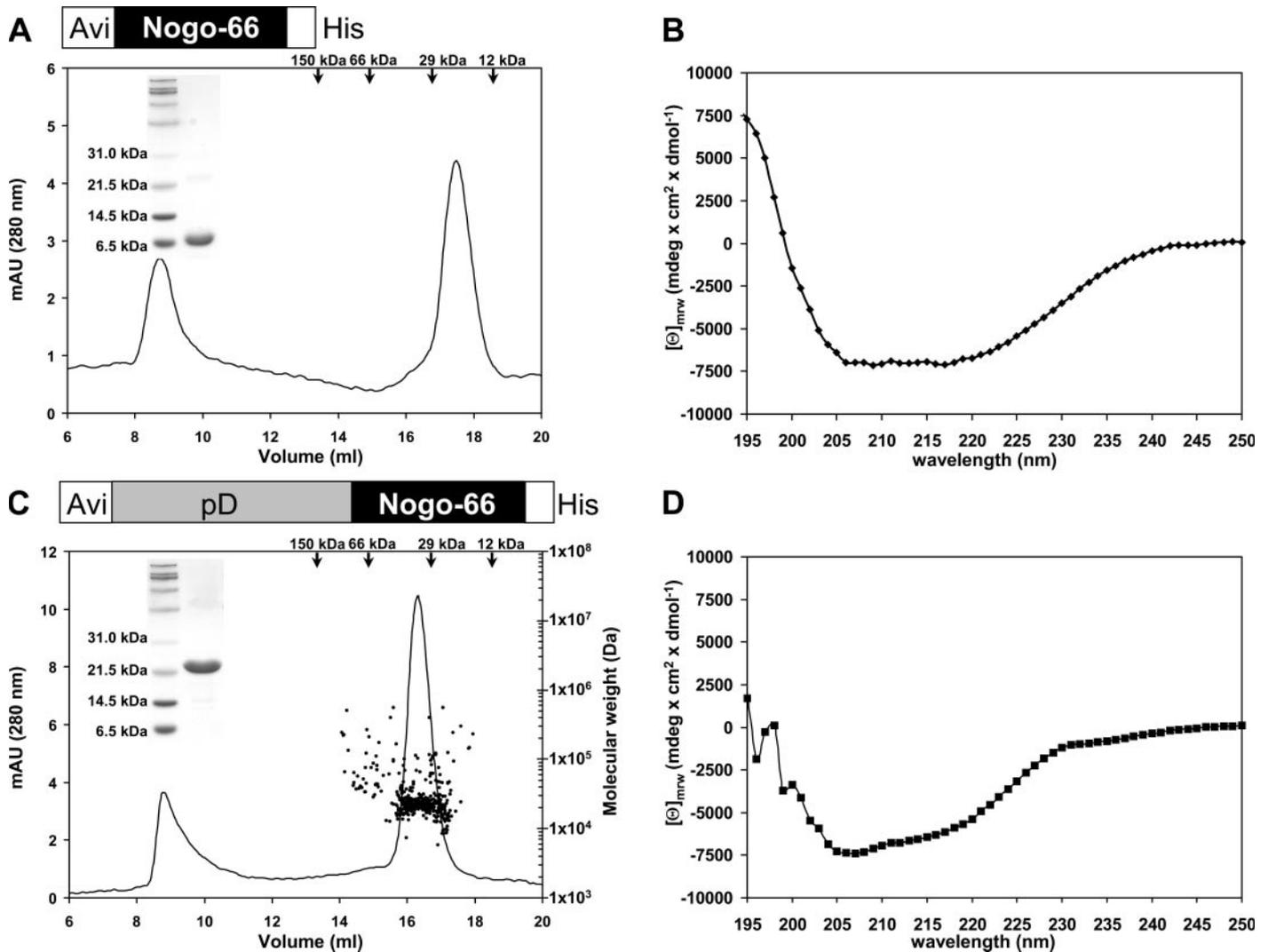
Fig. 1. Analysis of recombinant Nogo-66. (**A** and **B**) Nogo-66 with Avi- and His-tag, (**C** and **D**) pD–Nogo-66 fusion protein with Avi- and His-tag. The recombinant Nogo-66 fusion proteins are depicted schematically on top of the panels. (A and C) Size-exclusion chromatography of Nogo-66 constructs. Purified proteins were analysed by SDS–PAGE (15%) (inset), refolded by fast dilution into 50 mM Tris, 150 mM NaCl (pH 8.5), loaded on a Superdex 200 column and eluted with the same buffer. The A_{280} traces (left-hand axis) are shown. Gel filtration was followed by in-line multi-angle light scattering. Light scattering data converted to molecular mass are represented as clustered points for the pD–Nogo-66 fusion protein (right-hand axis). The average molecular mass of eluted pD–Nogo-66 is ∼23 kDa, corresponding to the mass of monomeric protein. (B and D) CD spectra for both proteins. Spectra were recorded at 4°C in borate buffer (pH 8.5).

Static light scattering and refractive index detection were performed in-line by a coupled miniDawn tri-angle light-scattering and an Optilab refractive index detector (Wyatt Technology). Molecular mass was calculated with a dn/dc value of 0.185.

Circular dichroism (CD) spectra

Experiments were performed on a J-715 spectropolarimeter (Jasco) at 4°C with 20 μM protein in 50 mM borate, 150 mM NaCl, pH 8.5 or the respective Tris-based buffer system using cuvettes with 1 mm pathlength. Data from four independent scans were averaged.

Binding studies

In vitro translations were carried out as described previously (Schaffitzel *et al.*, 2001) with addition of [^{35}S]methionine. After 10 min at 37°C, the translation reaction was stopped by 5-fold dilution with ice-cold WBK$_{500}$T buffer (50 mM Tris–acetate, pH 7.5, 150 mM NaCl, 50 mM magnesium acetate, 0.5 M KCl, 0.1% Tween-20) containing 2.5 mg/ml heparin. After centrifugation at 11 000 g for 5 min, the ternary complexes of RNA, ribosomes and protein were further purified by ultracentrifugation through a sucrose cushion. For this purpose, 500 μl of supernatant were applied to 2.5 ml of 35% sucrose in WBKT (50 mM Tris–acetate, pH 7.5, 150 mM NaCl, 50 mM magnesium acetate, 250 mM KCl, 0.1% Tween-20) and ultracentrifugation was carried out at 100 000 g for 20 min. The pellet was resuspended in WBKT and binding experiments were carried out in the presence of bovine serum albumin (BSA) (final concentration of 5 mg/ml) and *Saccharomyces cerevisiae* RNA (final concentration of 250 μg/ml). Equal amounts of ternary complexes were mixed with either WBKT or defined concentrations of Nogo-66 fusion protein in WBKT for competition. After shaking the mixture for 30 min at 4°C, 10^7 paramagnetic beads, coated with fusion proteins and equilibrated with WBKT, were added and the solution was shaken for 1 h at 4°C. For capturing ternary complexes via the N-terminal His-tag, mixtures were preincubated with 0.1 μg of

anti-RGS-His-tag antibody (Qiagen) and subsequently immobilized on Dynabeads containing immobilized protein G (Dynal Biotech). After incubation, the beads were washed five times with 0.8 ml of WBKT with a shaking period of 3 min between the washing steps. Bound complexes were then eluted with 8 M urea and quantified in a scintillation counter.

Gel electrophoresis of in vitro translations

For gel electrophoresis of translation products, *in vitro* translations were carried out for 25 min in the presence of [^{35}S]methionine. Release of protein from ternary complexes was achieved by adding 10-fold concentrated EDTA in Tris–HCl buffer (pH 7.5) to a final concentration of 20 mM or by adding 10-fold concentrated puromycin in the same buffer to a final concentration of 2 mM and an additional incubation for 5 min at 37°C. Soluble and insoluble fractions of 30 μl *in vitro* translation mix were separated by immediate centrifugation at 21 000 *g* for 5 min at 4°C. Acetone (120 μl) was added to the supernatant, incubated for 30 min on ice and centrifuged again. The pellet was dried and all fractions were resuspended in 27 μl of TBS. RNA was digested by adding 2 μl of 50 mM MgCl$_2$ and 1 μl of 1 mg/ml RNaseA and incubation for 20 min at 37°C. SDS loading buffer (15 μl) was added and, after heating, samples were subjected to reducing SDS gel electrophoresis on a 12% polyacrylamide gel.

Phage purification

Phagemids were transformed into *E.coli* XL1-Blue and grown on LB plates containing 1% glucose, 34 μg/ml chloramphenicol and 15 μg/ml tetracycline. A 5 ml volume of the same medium was inoculated with single colonies and grown at 37°C overnight. A 20 ml volume of 2YT medium containing 1% glucose, 34 μg/ml chloramphenicol and 15 μg/ml tetracycline was inoculated with the overnight culture and grown at 37°C to an A_{600} of 0.8. Then 10^{11} pfu VCS M13 helper phage (Stratagene) were added and the culture was incubated in a water-bath for 45 min at 37°C. After shaking for an additional 30 min at 37°C, the cells were centrifuged and the medium was replaced with 60 ml of 2YT containing 0.1 mM IPTG, 34 μg/ml chloramphenicol and 25 μg/ml kanamycin. The culture was shaken overnight at 30°C and phages were precipitated from the culture supernatant by incubation for 30 min with one-quarter volume of PEG–NaCl solution (20% PEG 6000, 2.5 M NaCl) on ice. The pellets were redissolved in PBS, pH 7.4, and precipitated once again with PEG–NaCl solution. After dissolution in PBS, phages were further purified by ultracentrifugation in a CsCl gradient as described (Bothmann and Plückthun, 1998).

Phage ELISA

Phage ELISAs to detect binding to Nogo-66 fusion protein were carried out under conditions similar to the binding assays with ribosomal complexes: 10^{12} phages in TBST (pH 7.5) were preincubated with or without ligand in the same buffer for 20 min and, after preincubation, paramagnetic beads coated with Nogo-66 fusion protein were added and incubated as described above. After washing, bound phages were detected with anti-M13-antibody conjugated with horseradish peroxidase (Pharmacia). Development was carried out by addition of 1:1 diluted BM Blue POD substrate (Roche) in PBST and the reaction was stopped by addition of 1 M H$_2$SO$_4$ after defined time periods.

Phage blots

Phage concentrations were determined spectrophotometrically; 1.5×10^{12} phages were subjected to a reducing 12% SDS–PAGE and blotted on a PVDF membrane (Immobilon-P, Millipore). Detection of g3p fusion proteins was carried out with primary antibodies mouse anti-FLAG M1 (Sigma), mouse anti-myc 9B11 (NEB) and the monoclonal antibody 10C3 recognizing the C-terminal domain of g3p (Tesar *et al*., 1995).

Results

Characterization of the Nogo-66 domain

The LRR portion of the Nogoreceptor has been shown to be necessary and sufficient for binding to the small extracellular domain of Nogo, termed Nogo-66 (Fournier *et al*., 2002). In order to probe the specific interaction of this part of Nogo with the Nogoreceptor expressed in a display system format, we first produced and characterized the recombinant Nogo-66 domain. We expressed Nogo-66 either alone with an N-terminal Avi-tag and a C-terminal His-tag or as a fusion to the C-terminus of various fusion partners. The proteins were all expressed as inclusion bodies in *E.coli* and purified by Ni-NTA affinity chromatography under denaturing conditions. Recently, Li *et al*. (2004) reported Nogo-66 to be insoluble in aqueous buffer. Even though we also found Nogo-66 to be highly aggregation prone and completely insoluble at neutral pH, the solubility of Nogo-66 increases markedly upon refolding and storage at higher pH values. Nogo-66 obtained by fast dilution refolding under conditions above pH 8.0 is soluble up to a concentration of 25 μM, independent of the buffer system employed. The presence of N-terminal fusion partners further increases the solubility of Nogo-66 and its half-life in solution. Figure 1 shows size-exclusion chromatographic profiles of (A) non-fused Nogo-66 and (C) Nogo-66 fused to protein D. While a certain fraction of refolded protein remains as soluble aggregates after refolding—eluting at the void volume of the column—~75% of pD–Nogo-66 and 65% of non-fused Nogo-66 elute as a single symmetric peak. The apparent molecular masses calculated from the elution volumes are 34.7 and 19.8 kDa, compared with theoretical values of 23.6 and 11.0 kDa, respectively. Even though these apparent molecular masses correspond to values only slightly below those of the respective homodimers, molecular mass determinations by static light scattering of the pD–Nogo-66 fusion result in a molecular mass of 22.9 ± 6.0 kDa (theoretical mass: 23.6 kDa), clearly indicating that the major fraction of refolded material is indeed monomeric. We were not able to obtain reliable light scattering data for non-fused Nogo-66, owing to its small molecular mass and the interference of the strong scattering signal of insoluble aggregates. However, the similar elution patterns and the fact that Nogo-66 complexed with the anti-Nogo-66 antibody alFv1 (see below) results only in complexes of 1:1 stoichiometry (data not shown) indicate that non-fused Nogo-66, like pD–Nogo-66, is monomeric. CD spectra of Nogo-66 (Figure 1B) show a broad negative feature from 205 to 220 nm, indicative of a significant proportion of α-helical secondary structure content in the protein. The measured spectra are independent of the buffer system used (phosphate, Tris or borate buffer). In agreement with the data of Li *et al*. (2004), Nogo-40, which only comprises the 40 N-terminal amino acids

of Nogo-66, was found to be unstructured under the same conditions (data not shown). Together, these data suggest that Nogo-66 may be the functional and structural unit necessary for forming a compact domain.

Constructs of the Nogoreceptor ligand binding domain for ribosome display and phage display

In order to examine whether the Nogoreceptor ligand binding domain can be displayed in an active form in a ribosome display or phage display format, the gene fragment encoding residues 24–331 of the Nogoreceptor (NR) was inserted into standard vectors for ribosome display and phage display (Figure 2A). For ribosome display, we used a C-terminal spacer sequence consisting of residues 20–109 of lambda phage capsid protein D (Forrer and Jaussi, 1998; Matsuura and Plückthun, 2003). For phage display, we used a phagemid system in which NR was placed behind a *phoA* signal sequence and fused to the C-terminal domain of the gene 3 protein of phage M13 (g3p). In both cases tags allow to detect the display of the respective fusion proteins.

The ligand binding domain of the Nogoreceptor contains two free cysteine residues in the LRR core region, in addition to the conserved disulfide bridges in the capping modules (Figure 2). LRR modules are defined by a unique consensus sequence and the consensus residues are responsible for the proper packing of the hydrophobic core (Kobe and Deisenhofer, 1995). Both free cysteine side chains in the LRR are buried and their positions correspond to positions of the LRR consensus motif that are otherwise almost exclusively occupied by leucine and asparagine, respectively. We were concerned that, in phage display, an illegitimate oxidation in the bacterial periplasm, en route to the phage coat, might covalently trap a misfolded structure and prevent its incorporation into the phage. In order to minimize this problem, Cys80 and Cys140 were mutated to the consensus residues Leu and Asn, respectively (Figure 2B). Because the LRR consensus motif is restored by these mutations, no negative influence on hydrophobic core packing or folding efficiency would be expected. Replacement of Cys140 by Asn is even likely to introduce an additional H-bond by completing the continuous arrangement of hydrogen bonds of the stacked asparagine side chains, commonly referred to as 'asparagine ladder' (Kobe and Deisenhofer, 1995), which connects the turns of neighbouring repeats. These constructs were then evaluated in ribosome display and phage display.

Ribosomal complexes of the Nogoreceptor are able to bind to its cognate ligand Nogo-66

The basis of a phenotypic selection for ligand binding is that the displayed protein can fold correctly into its native structure. Although no functional or soluble Nogoreceptor could so far be produced in the bacterial cytoplasm, periplasm or by refolding from inclusion bodies (data not shown), we found, surprisingly,
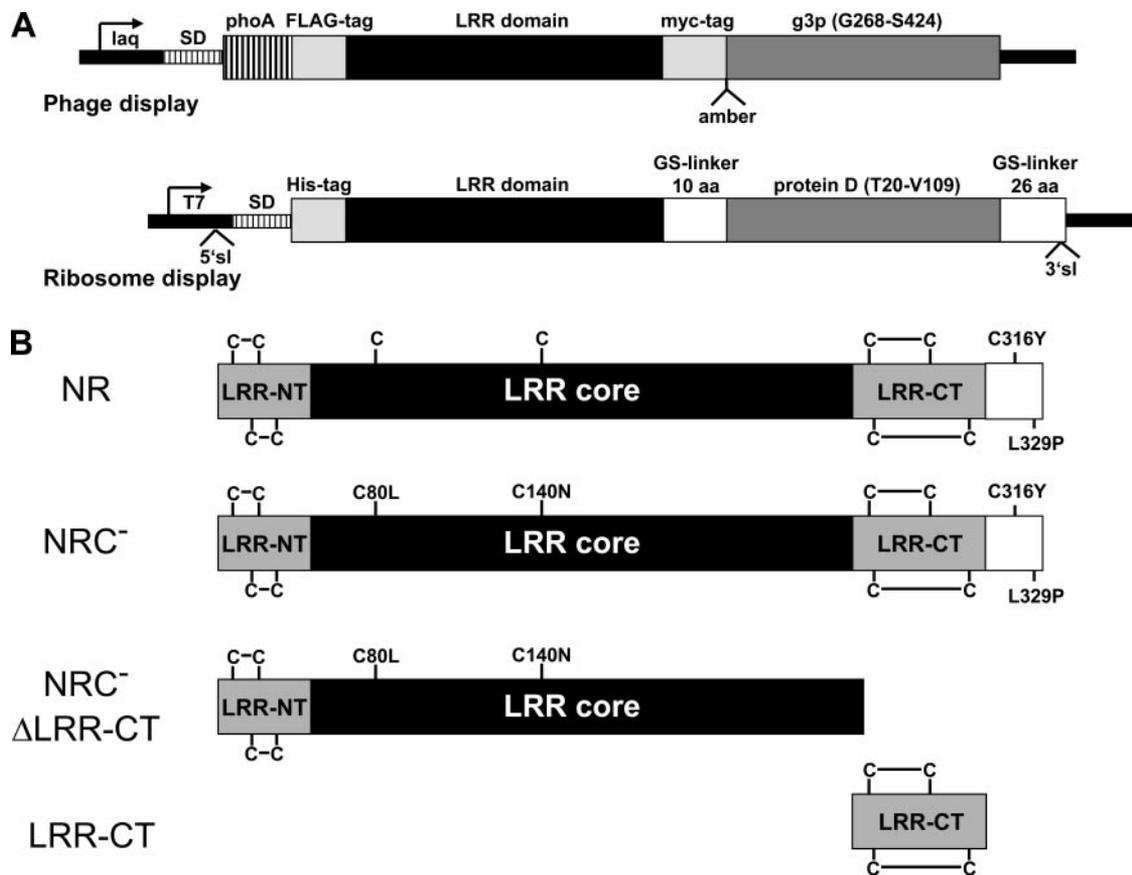

Fig. 2. (**A**) Schematic representation of the fusion constructs used for phage display (upper graph) and ribosome display (lower graph). (**B**) Schematic representation of variants of the Nogoreceptor ligand binding domain (residues 24–331) used in these studies. The conserved disulfide bridges in the N- and C-terminal 'capping modules' (LRR-NT, LRR-CT) and the free cysteines in the LRR core region are indicated. Both free cysteines are mutated to the respective consensus residues in variant NRC⁻. The LRR core region is composed of 8.5 LRR modules. The mutations in the far C-terminal overhang of 22 amino acids represent the changes of the macaque to the human receptor sequence.

that *in vitro* expression in the ribosome display format, with Nogoreceptor still bound to the ribosome, indeed yielded soluble ribosomal complexes displaying full-length Nogoreceptor domain. In order to test whether the displayed proteins are correctly folded and functional, we investigated the interaction of these ternary complexes with the cognate ligand Nogo-66. We established an assay in which Nogo-66 fusion proteins are immobilized on paramagnetic beads (M270-Epoxy, Dynal) and binding of ternary complexes is measured by radioimmunoassay (RIA) after *in vitro* translation of the Nogoreceptor domain in the presence of [^{35}S]methionine (Figure 3). Binding signals that are higher than background are only obtained on beads coated with Nogo-66 fusion proteins. Signals are significantly lower on beads that are coated with the same amount of fusion partner but missing the Nogo-66 portion or on beads that are coated with protein G, used as a control. In order to exclude that either ribosomes or RNA interact non-specifically with Nogo-66, we also checked the interaction of ribosomal complexes for which the Nogoreceptor domain is replaced with protein D or a soluble protein derived from a random sequence library (Matsuura and

Plückthun, 2003). Indeed, no binding was observed for ribosomes displaying these control proteins. Moreover, binding signals can be inhibited by the addition of free Nogo-66 fusion protein, clearly showing the ability of ternary complexes to interact with Nogo-66 both on the surface and in solution.

The observed IC$_{50}$ is ~2 μM (see below). In order to determine quantitatively the affinity between Nogoreceptor and Nogo-66 in this assay, the coating density of the ligand has to be chosen low enough to prevent shifting of the equilibrium in the liquid phase (Friguet *et al.*, 1985; Hetherington, 1990). Owing to the technical difficulties associated with the determination of the amount of immobilized ligand that is functionally active, and also the number of added ternary ribosomal complexes, we are not able to determine an accurate dissociation constant. Therefore, the measured IC$_{50}$ value measured in this assay solely represents an upper limit for K_D. Even so, the affinity seems still to be lower than the apparent affinities measured in cell-based assays, which were determined to be in the nanomolar range (Fournier *et al.*, 2001). Interestingly, the binding affinity also has been reported to be weaker in coimmunoprecipitation experiments with purified ligand
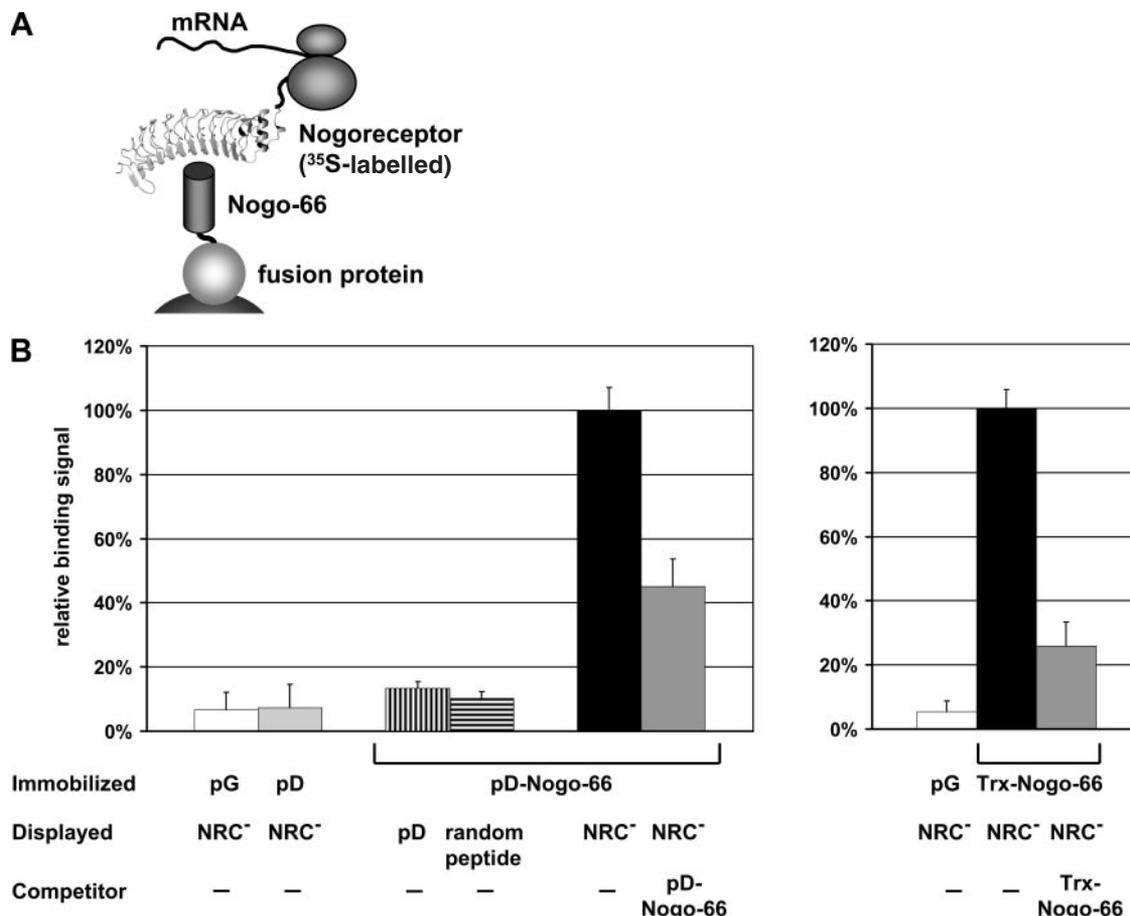

Fig. 3. RIA of ribosomal complexes displaying [^{35}S]methionine-labelled Nogoreceptor domains. (**A**) Schematic representation of the binding assay. (**B**) Binding of ribosomal complexes displaying *in vitro* translated and ^{35}S-labelled Nogoreceptor to Nogo-66 fusion proteins, immobilized on paramagnetic beads, was investigated. *Immobilized* refers to the protein coated on the magnetic beads, *displayed* to the protein translated and connected to the ribosomes and *competitor* to protein present in solution. As negative controls, the binding of Nogoreceptor-displaying ternary complexes to other proteins was investigated: binding to beads coated with protein G (white bars) or to beads coated with lambda phage protein D missing the C-terminal Nogo-66 insertion (light grey column). As further negative controls the non-specific binding of ribosomal complexes displaying unrelated proteins on immobilized pD–Nogo-66 was assessed: binding of ribosomal complexes only displaying protein D (vertically striped bars) or a protein derived from a random sequence library (horizontally striped lines). Black bars represent specific binding to Nogo-66, being immobilized either as a fusion to protein D or as a fusion to thioredoxin. Signals observed when the free ligand Nogo-66 is added as a competitor at a concentration of 4 μM (grey bars). All reactions were performed in the presence of 5 mg/ml BSA and 250 μg/ml *S.cerevisiae* RNA. Signals are normalized to the binding signal of the respective Nogo-66 fusion protein.

binding domain used for crystallization (He *et al.*, 2003). It should be noted, however, that cell binding assays on Nogoreceptor-displaying cells are crucially different from *in vitro* binding assays on immobilized Nogo-66 ligand. Like the purified ligand binding domain, Nogoreceptor displayed on ribosomes is most likely monomeric, resulting in a binding stoichiometry of 1:1. In contrast, multimerization has been shown to occur for GPI-linked Nogoreceptor on the cell surface (Fournier *et al.*, 2002), which most likely leads to avidity effects that will have a drastic influence on the apparent K_D. Importantly, our results also show that the non-glycosylated LRR core protein of the Nogoreceptor is sufficient to mediate binding to Nogo-66.

Nogoreceptor is not amenable to phage display

In contrast to the results obtained with ribosome display, M13 phages produced in cells harbouring phagemid vectors encoding the Nogoreceptor domain which is fused to the C-terminal part of g3p showed no specific binding to Nogo-66 immobilized on paramagnetic beads, as determined by phage ELISA (Figure 4A). As a positive control, the single-chain Fv (scFv) fragment aIFv1 was used, which we selected previously to bind specifically to Nogo-66 (B.Schimmele, unpublished results) obtained by phage panning with the fully synthetic Human Combinatorial Antibody Library (HuCAL) (Knappik *et al.*, 2000). The high sensitivity of phage ELISA (because of the signal amplification inherent in anti-p8 antibodies) allows even the detection of low-affinity binding and a small number of phages displaying functional protein, suggesting almost a complete absence of functional Nogoreceptor. For the functional display on phages, proteins have to be transported to the periplasmic space, where protein folding of g3p fusions occurs in a

membrane-bound state prior to incorporation into the phage. In the monovalent phage display system used, wild-type g3p from the helper phage competes with the g3p fusion proteins for incorporation into the phage particles, ensuring that phages are properly assembled and infectivity is maintained. As a result, phage titres are usually independent of the displayed protein. The display level, i.e. the amount of fusion protein incorporated in the phage coat is dependent, at least partly, on the amount of correctly folded protein in the periplasm (Bothmann and Plückthun, 1998). We used tags, placed N- and C-terminally of the NR domain, to check whether the LRR protein is indeed displayed on the phage. Whereas the control scFv is detected by antibodies directed against both tags, neither variant of the Nogoreceptor domain can be detected (Figure 4B). This lack of incorporation into the phage is most likely caused by severe aggregation of the translated fusion protein prior to phage assembly, either in the periplasm or perhaps even before the transport through the inner membrane. Hence phage display cannot be used for these receptor domains.

Ribosomal complexes provide a favourable environment for the folding and functional display of Nogoreceptor

Different reasons could account for the soluble expression of NR in active form in the ribosome display format. Even though the presence of eukaryotic protein disulfide isomerase (PDI) in the translation mix might be crucial for the formation of correct disulfide bridges and prevent aggregation upon misfolding or formation of intermolecular disulfides, translation in the absence of PDI or under different redox conditions did not result in either a significant decrease in soluble ternary complexes or in a significant reduction of binding to pD–Nogo-66 (data not shown), indicating that the formation of disulfide
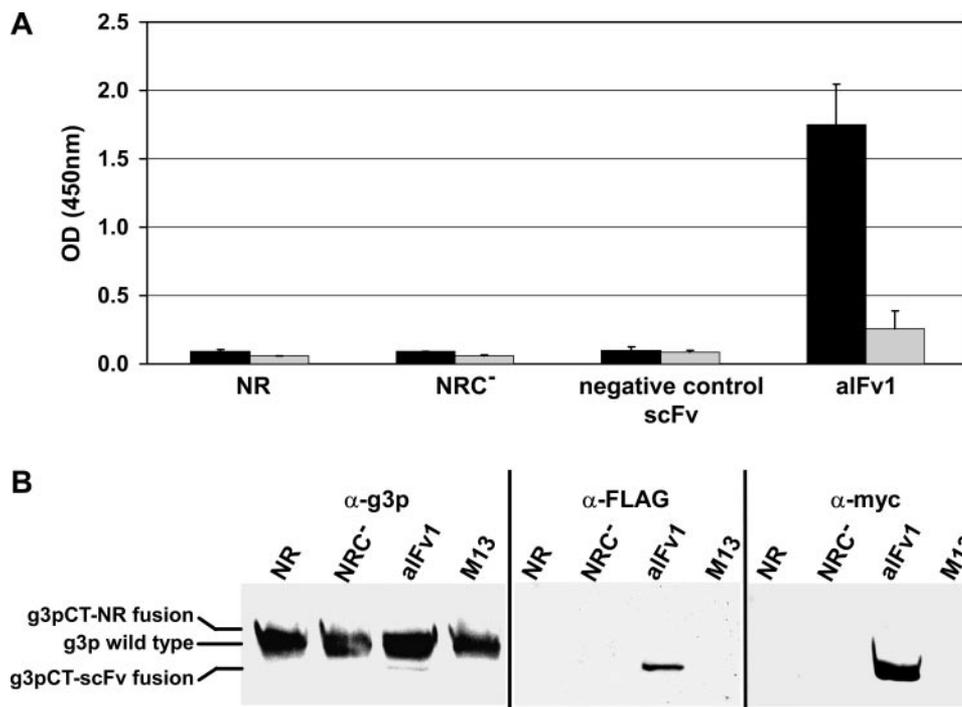

Fig. 4. (**A**) Phage ELISA on paramagnetic beads coated with pD–Nogo-66. Black bars represent binding of phage and grey columns binding of phages in the presence of 4 μM pD–Nogo-66 as competitor. As a negative control, phages displaying an unrelated scFv antibody were used. (**B**) Phage blot. Detection of the indicated g3p fusion proteins displayed on phages; 1.5×10^{11} phages were applied per lane and detected either with an antibody directed against the C-terminal domain of g3p (left panel) or with antibodies detecting only the fusion proteins via the fused tags (middle and right panels).

bridges in the capping modules is not crucial for attaining a native-like conformation of the LRR portion of the domain. Several observations indicate instead that in fact the tethering of proteins to the ribosome and RNA is the major reason why aggregation is prevented.

Previously, it had been observed that a protein derived from a random sequence library with a strong tendency to form amyloid-like fibrils still resulted in soluble ternary complexes, suggesting that the ribosome and the connected RNA can act as solubility-enhancing fusion partners and may sterically block aggregation (Matsuura and Plückthun, 2003). We therefore wanted to test whether the solubility of *in vitro* translated receptor domains is directly linked to their presence in ternary complexes. Disintegration of ternary complexes can be achieved by adding either EDTA or puromycin, leading to a release of translated protein from the ribosome. After defined times of translation, EDTA-containing buffer of the same pH was added to the translation mix, briefly incubated and aggregated protein was collected by centrifugation. Upon addition of EDTA, a strong increase in the amount of aggregated receptor and an equivalent decrease in the amount of soluble receptor can be observed for *in vitro* translated Nogoreceptor and also for *in vitro* translated biglycan, a domain of similar structure (Figure 5). Upon addition of puromycin, a strong effect on the solubility of *in vitro* translated biglycan is observed, but effects on the solubility of displayed Nogoreceptor are small (data not shown). In contrast, control proteins which are not aggregation prone remain in solution upon addition of either reagent. These data suggest that aggregation indeed occurs to a certain degree post-translationally upon protein release from the ribosome. In addition, expression in the context of ribosomal complexes allowed the soluble display of other aggregation-prone receptor domains, such as the extracellullar domain of the luteinizing hormone receptor or decorin (data not shown), suggesting that these observations represent a general feature of ribosome display. The potential of the ribosome to act as a
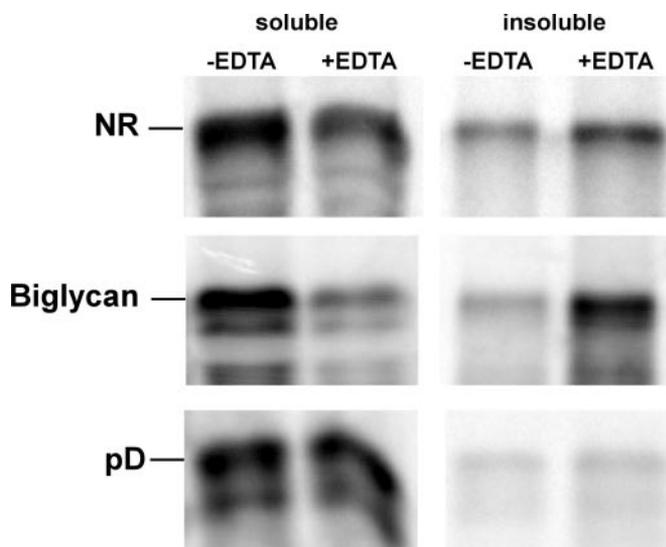

Fig. 5. *In vitro* translation of ribosome display constructs encoding the Nogoreceptor domain, biglycan core protein or protein D as a soluble control protein. After 25 min of translation, EDTA was added to release translated proteins from the ribosome and the sample was incubated for an additional 5 min. Soluble and insoluble fractions were separated by immediate centrifugation at 4°C, treated as described in Materials and methods and analysed by SDS gel electrophoresis and autoradiography.

solubility-enhancing fusion partner has also been used in covalent coupling of inclusion body-forming proteins to the ribosome in order to make them soluble (Sorensen *et al.*, 2004). It is noteworthy that aggregation is not quantitative and a certain fraction of protein remains in solution even after EDTA-induced release from ribosomal complexes. Hence it is possible that the aggregating portion simply represents the fraction which has not attained the correct native fold, while the remaining soluble fraction has folded into a native-like structure, while being forced to stay out of contact with other receptor molecules. As non-productive intermolecular interactions leading to aggregation and productive intramolecular interactions responsible for attaining the native structure compete with each other, the longer persistence of the protein in ternary complexes—compared with the situation *in vivo*—could enable the polypeptide chain to acquire a native-like fold before intermolecular interactions and subsequent aggregation occur.

Binding studies with the displayed Nogoreceptor domain

We first wanted to check whether the introduced consensus mutations substituting the free cysteines in the LRR core region would have any influence on the display rate or the affinity of the displayed domain. By direct comparison with the wild-type, we observed a slight increase in the display rate (1.5-fold) of NRC$^-$ as judged by the number of soluble complexes captured by an anti-His-tag antibody with subsequent immuno-precipitation on paramagnetic beads coated with protein G (Figure 6A). The inhibition patterns of both variants do not display significant differences (Figure 6B), showing that the consensus mutations do not disturb the binding of ternary complexes to Nogo-66.

The specific binding mode of Nogo-66 on the LRR domain of the Nogoreceptor is still unclear and controversial. In cell-based assays with deletion mutants of the Nogoreceptor, weak binding activity of the LRR-CT region alone, but no binding activity of a construct comprising only LRR-NT and the LRR core, has been reported (Wang *et al.*, 2002). A larger series of deletion mutants has been investigated by Fournier *et al.* (2002), in which capping modules and any two adjacent repeat modules were deleted at a time. However, no binding was detected for any of the deletion mutants and the authors concluded that binding activity is dispersed over the LRR domain. Nevertheless, as mentioned previously, effects of receptor multimerization or interactions with coreceptor might have a strong influence on the binding activity measured in cell-based assays.

We therefore tested whether binding activity can be detected for LRR-CT alone or, conversely, deletion of LRR-CT will lead to a drastic reduction in binding activity towards Nogo-66 in our *in vitro* assay. In accordance with the results of Wang *et al.* (2002), we are able to detect weak binding activity for the C-terminal capping module alone. However, in contrast to the results of Fournier *et al.* (2002), deletion of LRR-CT does not lead to a severe decrease in the binding signal (Figure 7), showing that indeed the LRR core region makes the major contribution to the binding to Nogo-66.

Discussion

We have expanded the applicability of ribosome display to mammalian receptor domains. Despite the high tendency of
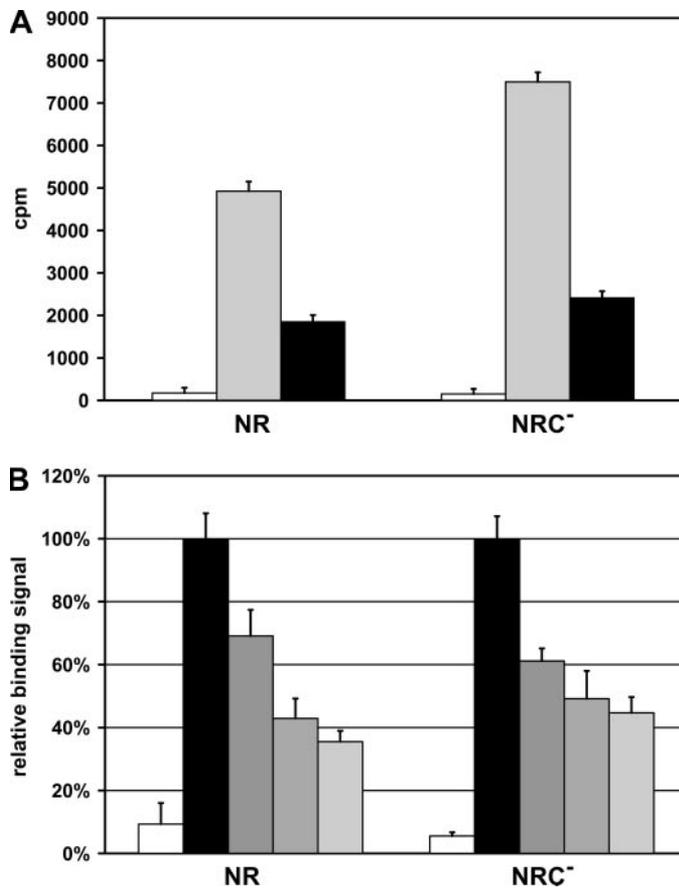
Fig. 6. (**A**) Display rate and binding to Nogo-66 of ribosomal complexes displaying NR and NRC⁻. White bars represent background binding to protein G. Grey bars represent the signal upon immunoprecipitation of ribosomal complexes with anti-His antibody on protein G beads. Black bars represent binding on pD–Nogo-66-coated epoxy beads. (**B**) Competition RIA. Inhibition patterns of ribosomal complexes displaying variants NR and NRC⁻. White bars represent background binding to protein G. Black bars represent binding to pD–Nogo-66 and grey bars inhibition of binding by addition of 1, 4 and 10 µM pD–Nogo-66.

Fig. 7. Binding of truncated versions of the Nogoreceptor in comparison with the full-length receptor domain (NRC⁻). Binding signals are represented as black bars, the signal upon addition of 4 µM free ligand as competitor to the solution is represented by grey bars and non-specific binding of ribosomal complexes to protein G is shown as white bars. NRC⁻ΔCT comprises residues 24–260 of the ligand binding domain missing the C-terminal flanking region. CT comprises residues 261–314 representing only the C-terminal flanking region.

these protein domains to form insoluble aggregates upon heterologous expression in *E.coli*, both in the cytoplasm and the periplasm and upon refolding from inclusion bodies *in vitro*, they can apparently fold while still held by the ribosome. Many cell surface receptors, including the Nogoreceptor, are glycosylated. Several observations indicate active roles of glycan side chains for protein folding, such as facilitating interactions with certain folding modulators (Trombetta and Helenius, 1998), increasing the solubility of native state proteins and presumably folding intermediates or even increasing the thermodynamic stability of the native state (Giraud *et al.*, 1992; van Zuylen *et al.*, 1997). It is therefore an intriguing hypothesis that the ribosome display format, with the RNA and the ribosome still connected to the nascent polypeptide, might provide a similar environment which enhances the solubility of partially folded species or even sterically blocks the aggregation of displayed proteins. If folding needs to proceed over a comparatively long time-scale, this environment might allow the protein to acquire a native-like fold before intermolecular interactions and subsequent aggregation occur. This special environment in ternary complexes, being composed of the receptor, the ribosome and RNA, allows the soluble and functional expression in a conventional *in vitro* translation set-up, provided that the mRNA has no stop codon, the solution is
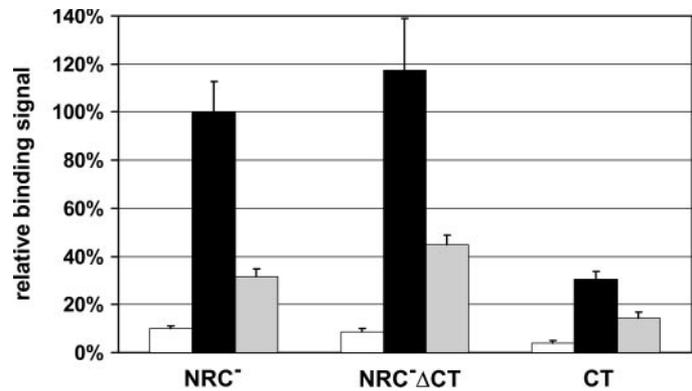
cooled and the ribosome is stabilized by a suitable buffer. This approach now allows us to test rapidly mutants *in vitro* when the pure recombinant protein is otherwise inaccessible or can only be obtained from mammalian production. Furthermore, this should make it possible to evolve variants of the Nogoreceptor with higher affinity, stability or solubility (Jermutus *et al.*, 2001; Matsuura and Plückthun, 2003). Even though phage display represents another versatile tool for evolving proteins towards higher stability (Jung *et al.*, 1999) or higher resistance to aggregation (Jespers *et al.*, 2004), this methodology is limited to proteins that can be functionally displayed on filamentous phage. Other important applications include combinatorial approaches to identify and dissect residues important for binding (Weiss *et al.*, 2000). Therefore, the ternary complexes in ribosome display allow the folding of aggregation-prone proteins *in vitro* and to make such proteins accessible to analytical dissection and an evolutionary improvement.

Besides the previously mentioned advantages of the ribosome display technology such as large library sizes and the powerful built-in evolution process, our results suggest that ribosome display can also be a versatile analytical tool for aggregation-prone proteins and other mammalian receptor molecules whose binding activity is not directly dependent on post-translational modifications. This system does not only allow the investigation of structure–function relationships in a combinatorial way, but has the potential to evolve receptor domains with properties more suitable for drug-related applications. Such engineered variants of the Nogoreceptor domain may be useful as therapeutic agents for treating spinal chord injuries, stroke or traumatic head injuries.

Acknowledgements

References

Binz,H.K., Amstutz,P., Kohl,A., Stumpp,M.T., Briand,C., Forrer,P., Grütter,M.G. and Plückthun,A. (2004) *Nat. Biotechnol.*, **22**, 575–582.
Bothmann,H. and Plückthun,A. (1998) *Nat. Biotechnol.*, **16**, 376–380.
Chen,M.S., Huber,A.B., van der Haar,M.E., Frank,M., Schnell,L., Spillmann,A.A., Christ,F. and Schwab,M.E. (2000) *Nature*, **403**, 434–439.

Dunn,I.S. (1996) *Curr. Opin. Biotechnol.*, **7**, 547–553.

Ellgaard,L., Molinari,M. and Helenius,A. (1999) *Science*, **286**, 1882–1888.

Forrer,P. and Jaussi,R. (1998) *Gene*, **224**, 45–52.

Fournier,A.E., GrandPre,T. and Strittmatter,S.M. (2001) *Nature*, **409**, 341–346.

Fournier,A.E., Gould,G.C., Liu,B.P. and Strittmatter,S.M. (2002) *J. Neurosci.*, **22**, 8876–8883.

Friguet,B., Chaffotte,A.F., Djavadi-Ohaniance,L. and Goldberg,M.E. (1985) *J. Immunol. Methods*, **77**, 305–319.

Giraud,A., Franc,J.L., Long,Y. and Ruf,J. (1992) *J. Endocrinol.*, **132**, 317–323.

GrandPre,T., Nakamura,F., Vartanian,T. and Strittmatter,S.M. (2000) *Nature*, **403**, 439–444.

Hanes,J. and Plückthun,A. (1997) *Proc. Natl Acad. Sci. USA*, **94**, 4937–4942.

He,X.L., Bazan,J.F., McDermott,G., Park,J.B., Wang,K., Tessier-Lavigne,M., He,Z. and Garcia,K.C. (2003) *Neuron*, **38**, 177–185.

Hering,T.M., Kollar,J., Huynh,T.D. and Varelas,J.B. (1996) *Anal. Biochem.*, **240**, 98–108.

Hetherington,S. (1990) *J. Immunol. Methods*, **131**, 195–202.

Jermutus,L., Honegger,A., Schwesinger,F., Hanes,J. and Plückthun,A. (2001) *Proc. Natl Acad. Sci. USA*, **98**, 75–80.

Jespers,L., Schon,O., Famm,K. and Winter,G. (2004) *Nat. Biotechnol.*, **22**, 1161–1165.

Jung,S., Honegger,A. and Plückthun,A. (1999) *J. Mol. Biol.*, **294**, 163–180.

Knappik,A., Ge,L., Honegger,A., Pack,P., Fischer,M., Wellnhofer,G., Hoess,A., Wölle,J., Plückthun,A. and Virnekäs,B. (2000) *J. Mol. Biol.*, **296**, 57–86.

Kobe,B. and Deisenhofer,J. (1995) *Curr. Opin. Struct. Biol.*, **5**, 409–416.

Kobe,B. and Kajava,A.V. (2001) *Curr. Opin. Struct. Biol.*, **11**, 725–732.

Li,M., Shi,J., Wei,Z., Teng,F.Y., Tang,B.L. and Song,J. (2004) *Eur. J. Biochem.*, **271**, 3512–3522.

Lobel,L., Pollak,S., Lustbader,B., Klein,J. and Lustbader,J.W. (2002) *Protein Expr. Purif.*, **25**, 124–133.

Matsuura,T. and Plückthun,A. (2003) *FEBS Lett.*, **539**, 24–28.

McGee,A.W. and Strittmatter,S.M. (2003) *Trends Neurosci.*, **26**, 193–198.

Miroux,B. and Walker,J.E. (1996) *J. Mol. Biol.*, **260**, 289–298.

Schaffitzel,C., Zahnd,C., Amstutz,P., Luginbühl,B. and Plückthun,A. (2001) In Golemis,E. (ed.), *Protein–Protein Interactions. A Molecular Cloning Manual*. Cold Spring Harbor Laboratory Press, Cold Spring Harbor, NY, pp. 535–567.

Sorensen,H.P., Kristensen,J.E., Sperling-Petersen,H.U. and Mortensen,K.K. (2004) *Biochem. Biophys. Res. Commun.*, **319**, 715–719.

Tesar,M., Beckmann,C., Rottgen,P., Haase,B., Faude,U. and Timmis,K.N. (1995) *Immunotechnology*, **1**, 53–64.

Trombetta,E.S. and Helenius,A. (1998) *Curr. Opin. Struct. Biol.*, **8**, 587–592.

van Zuylen,C.W., Kamerling,J.P. and Vliegenthart,J.F. (1997) *Biochem. Biophys. Res. Commun.*, **232**, 117–120.

Wang,K.C., Kim,J.A., Sivasankaran,R., Segal,R. and He,Z. (2002) *Nature*, **420**, 74–78.

Weiss,G.A., Watanabe,C.K., Zhong,A., Goddard,A. and Sidhu,S.S. (2000) *Proc. Natl Acad. Sci. USA*, **97**, 8950–8954.

Wormald,M.R. and Dwek,R.A. (1999) *Struct. Fold. Des.*, **7**, R155–R160.

Wyss,D.F., Choi,J.S., Li,J., Knoppers,M.H., Willis,K.J., Arulanandam,A.R., Smolyar,A., Reinherz,E.L. and Wagner,G. (1995) *Science*, **269**, 1273–1278.

Yang,F., Forrer,P., Dauter,Z., Conway,J.F., Cheng,N., Cerritelli,M.E., Steven,A.C., Plückthun,A. and Wlodawer,A. (2000) *Nat. Struct. Biol.*, **7**, 230–237.